

Original Research

Excess Ub-K48 Induces Neuronal Apoptosis in Alzheimer's Disease

Qiang Li^{1,†}, Yiyuan Yuan^{2,†}, Shi Huang^{2,†}, Guangfu Di³, Haoyuan Chen⁴, Yani Zhuang², Wanzhen Fang⁵, Yanjiao Huang¹, Yinan Tao¹, Jing Jiang^{1,*}, Zhiliang Xu^{6,7,*}

Academic Editors: Changjong Moon and Bettina Platt

Submitted: 18 July 2024 Revised: 14 September 2024 Accepted: 20 September 2024 Published: 24 December 2024

Abstract

Background: K48-linked ubiquitin chain (Ub-K48) is a crucial ubiquitin chain implicated in protein degradation within the ubiquitinproteasome system. However, the precise function and molecular mechanism underlying the role of Ub-K48 in the pathogenesis of Alzheimer's disease (AD) and neuronal cell abnormalities remain unclear. The objective of this study was to examine the function of K48 ubiquitination in the etiology of AD, and its associated mechanism of neuronal apoptosis. Methods: A mouse model of AD was constructed, and behavioral phenotypic changes were detected using an open field test (OFT). The expression of glial fibrillary acidic protein (GFAP), an early marker of AD, was detected by western blotting (WB). Neuronal apoptosis in the hippocampal region was assessed by hematoxylin and eosin (HE) and Nissl staining. Immunohistochemistry and immunofluorescence were performed to observe the changes in Phosphorylated tubulin associated unit (p-Tau) and Ub-K48 colocalization in neurons of the hippocampal region of AD mice. WB was further applied to detect the degree of ubiquitylation of K48 and the expression of Tau, p-Tau, B-cell lymphoma-2 (Bcl-2) and Bcl-2-associated X (Bax) proteins in neuronal cells of the hippocampus and cortical regions of mice. Results: Mice with AD exhibited significantly longer resting times (p < 0.05) and shorter average speeds (p < 0.01), total distances travelled (p < 0.01), and distances travelled (p < 0.01) in the central region than those in the control group. This indicated cognitive impairment, which occurred concurrent with an increased expression of the AD marker GFAP protein (p < 0.001). The hippocampal region of AD mice showed abnormalities with sparsely and irregularly arranged cells, large gaps between cells, lighter staining, unclear boundaries of the cell membranes and nuclei, and agglutinated and condensed nuclei (p < 0.01). The neuronal cells of AD mice exhibited significantly elevated levels of p-Tau (p < 0.01) and Ub-K48 (p < 0.01), as well as a notable degree of co-localization within the cells. The intracellular pro-inflammatory protein Bax was significantly upregulated (p < 0.05), while the Bcl-2/Bax ratio was significantly lower than that in the control group (p < 0.05), thus inducing apoptosis in AD neuronal cells. **Conclusion**: Ub-K48 is strongly linked to the development of AD. p-Tau aggregate in neuronal cells in the hippocampal region of the AD brain and colocalize with Ub-K48, which in turn leads to cellular inflammation and the induction of apoptosis in neuronal cells.

Keywords: Alzheimer's disease; Ub-K48; p-Tau; apoptosis

1. Introduction

Alzheimer's disease (AD) is a prevalent neurodegenerative disorder that significantly impairs the physical and mental health of the elderly, severely impacting quality of life. As the global population continues to age, AD has emerged as a significant public health concern for governments worldwide [1]. It is estimated that by 2050, more than 130 million individuals will develop AD globally [2]. However, the cause of AD remains unclear, and its pathogenesis is complex. Pathologically, AD is characterized by the formation of senile plaques (SP) in the brain tissue, which comprise deposits of amyloid β peptide (A β). Neu-

rofibrillary tangles (NFTs) are formed by the hyperphosphorylation of intracellular Tau.

Impairment of the ubiquitin-proteasome system (UPS), a major pathway for protein degradation, can result in the aberrant aggregation of phosphorylated Tau (p-Tau) [3]. In certain instances, the accumulation of aberrantly aggregated proteins exceeds the degradation capacity of the ubiquitin-proteasome system, which can result in the abnormal accumulation of ubiquitinated proteins, thereby inducing neuronal dysfunction or apoptosis [4]. The inhibition of 26S proteasome activity in dopaminergic neurons in the substantia nigra of mice further results

¹Human Anatomy Experimental Training Center, School of Basic Medical Sciences, Wannan Medical College, 241002 Wuhu, Anhui, China

²School of Clinical Medicine, Wannan Medical College, 241002 Wuhu, Anhui, China

³Department of Neurosurgery, Anhui Digital Brain Engineering Research Center, The First Affiliated Hospital of Wannan Medical College, Yijishan Hospital of Wannan Medical College, 241001 Wuhu, Anhui, China

⁴School of Nursing, Wannan Medical College, 241002 Wuhu, Anhui, China

⁵School of Stomatology, Wannan Medical College, 241002 Wuhu, Anhui, China

⁶Department of Human Anatomy, School of Basic Medical Sciences, Wannan Medical College, 241002 Wuhu, Anhui, China

⁷Anhui Province Key Laboratory of Basic Research and Translation of Aging-Related Diseases, Wannan Medical College, 241002 Wuhu, Anhui, China

^{*}Correspondence: xuzhiliang@wnmc.edu.cn; xuzhiliang2010@foxmail.com (Zhiliang Xu); 2399221527@qq.com (Jing Jiang)

[†]These authors contributed equally.

in the development of the pathological manifestations of Parkinson's disease (PD), including apoptosis of dopaminergic neurons and formation of Lewy body (LB) inclusions [5]. The incidence of mitochondrial DNA loss in LB-positive neurons in PD brains is higher than that in LB-negative neurons, indicating that mitochondrial damage is increased in LB-positive neurons, which is a direct indication that the abnormal function of the UPS system plays an important role in the pathogenesis of neurodegenerative diseases [6,7]. This suggests that multiple proteases within the ubiquitin-proteasome system are closely linked to dopamine neuron function, and that their mechanisms of action and substrate recognition patterns are of broad biological and clinical significance, providing a new avenue for investigating the pathogenesis of neurodegenerative diseases. Furthermore, ubiquitin and certain proteasome subunits have been found in SP and NFTs, further suggesting that dysfunction of the ubiquitin protease system may be an important factor contributing to AD pathogenesis [8].

The K48 ubiquitin chain (Ub-K48) is a crucial form of substrate labeling for proteasomal degradation. This chain serves as a signal for proteasomal degradation and its dysfunction is directly related to the degradation of numerous proteins. It has been demonstrated that USP9X/USP24 promotes cell survival by removing Ub-K48 from Myeloid cell leukemia 1 (MCL-1), which has been identified as an essential survival factor in midbrain dopaminergic neurons [9,10]. However, whether Ub-K48 affects p-Tau accumulation in patients with AD remains unclear. Apoptosis is a ubiquitous physiological phenomenon in eukaryotic cells that is typically accompanied by the transport of aberrant proteins and organelles to the lysosomes for degradation. A decrease in the dopaminergic neuronal marker protein TH, and an increase in the levels of Ub-K48 have been observed in clinical PD case reports, as well as in animal and cellular models. Furthermore, some studies have reported that intrinsic apoptosis plays an important role in neurodegenerative lesions, particularly driving neuronal loss by inducing apoptosis [11-13]. As such, it is imperative to investigate the functional role of Ub-K48 in neuronal apoptosis during AD progression.

Although numerous studies have reported the involvement of K48 in the progression of degenerative neurological diseases, the mechanism underlying K48 ubiquitination during AD progression has not yet been reported. In this study, we successfully constructed an aging mouse model of AD and observed that p-Tau, accompanied by K48 polyubiquitination, was highly expressed in neuronal cells in the hippocampal region, showing significant overlap in terms of intracellular localization. This induces cellular inflammatory responses and the expression of the proinflammatory protein Bax in large quantities, which ultimately promoted the apoptosis of neuronal cells.

2. Materials and Methods

2.1 Experimental Animals

Male C57BL/6 mice (Jinan Pengyue, Jinan, Shandong, China) were used for this study under the animal production license SCXK(LU)2019-0003. The rearing environment was conducive to maintaining a stable room temperature and humidity, with natural ventilation, circadian rhythm, and unrestricted access to food and water. The operation and treatment of mice during the experiment adhered to the guidelines and ethical regulations of the Wannan Medical College on the humane treatment of animals. The animal ethics review number was WNMC-AWE-2023132.

2.2 Reagents and Antibodies

Radioimmunoprecipitation assay buffer (RIPA) lysate (Beyotime, P0013C, Shanghai, China); phenylmethanesulfonylfluoride (PMSF) (Beyotime, ST2573, Shanghai, China); 5×SDS sampling buffer (Beyotime, P0015L, Shanghai, China); Glial fibrillary acidic protein (GFAP) antibody (CST, #3670, Danvers, MA, USA); p-Tau antibody (Invitrogen, MN1020, Carlsbad, CA, USA); Tau antibody (Abcam, ab308439, Cambridge, UK); Ub-K48 antibody (Millipore, 05-1307, Bedford, MA, USA); Bcell lymphoma-2 (Bcl-2) antibody (Proteintech, 68103-1-Ig, Rosemont, IL, USA); Bcl-2-associated x protein (Bax) antibody (Proteintech, 50599-2-Ig, Rosemont, IL, USA); β -Actin antibody (Beyotime, AF5003, Shanghai, China); glyceraldehyde-3-phosphate dehydrogenase (GAPDH) antibody (Biosharp, BL006B, Hefei, Anhui, China); Goat anti-rabbit IgG (Beyotime, A0208, Shanghai, China); Goat anti-mouse IgG (Beyotime, A0216, Shanghai, China); Hematoxylin stain (Phygene, LA0516, Fuzhou, Fujian, China); Eosin stain (Phygene, BA-4098, Fuzhou, Fujian, China); Nissl stain (Servicebio, G1036, Wuhan, Hubei, China); Immunohistochemistry kit (OriGene, Sp-9000, Rockville, MD, USA).

2.3 Animal Model Preparation and Anesthesia

Specific Pathogen Free (SPF)-grade, 71-week-old, senescent male C57B/L6 mice (Weight: 31–36 g) were screened for open field test (OFT) behavioral identification as an AD model, while 5-week-old healthy mice (Weight: 16–21 g) were used as controls. The mice were anesthetized with 1% pentobarbital sodium (Yacoo, W0091, Suzhou, Jiangsu, China), injected intraperitoneally at 15 mg/kg of body weight and subsequently sacrificed by cervical dislocation. The skull was then peeled off to remove the brain tissue, which was subsequently divided into two equal parts for the cryogenic isolation of the hippocampal tissues. One portion was immersed in a 4% paraformaldehyde solution and stored in a refrigerator at 4 °C, while the other portion was placed in a –80 °C refrigerator for subsequent experiments.



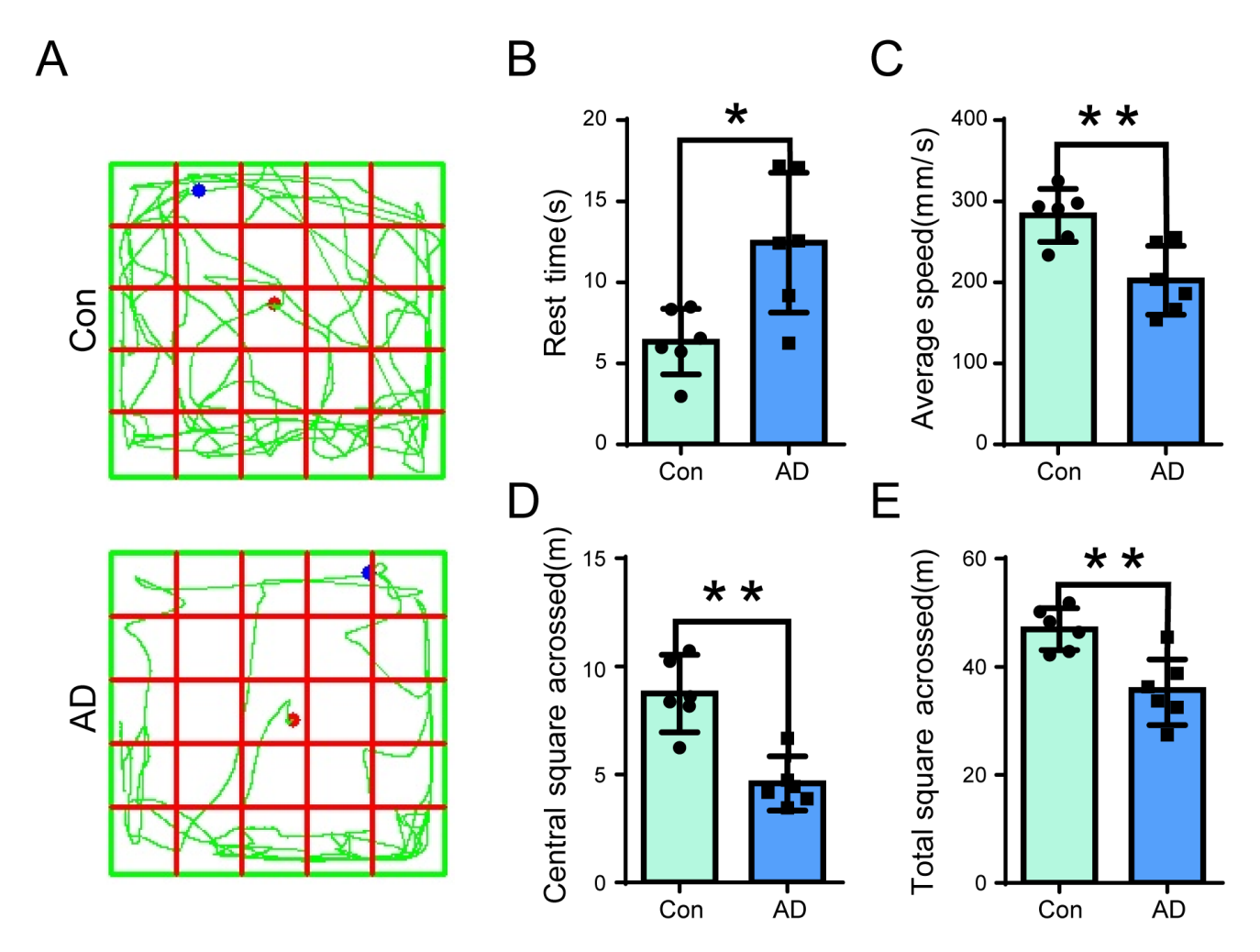


Fig. 1. Open-field test (OFT) assay in Alzheimer's disease (AD) mice. (A) Open field behavioral tests were conducted on control (Upper panel) and AD (Lower panel) mice, to record the resting time, average speed, total distance travelled, and distance travelled in the central region. (B–E) The resting time (B) of AD mice was significantly longer than that of the control group (n = 6, p < 0.05), while the average speed (C) (n = 6, p < 0.01), distance travelled in the central region (D) (n = 6, p < 0.01), and total distance travelled (E) (n = 6, p < 0.01) of AD mice were significantly shorter than that of the control group. Significance symbols indicate: *p < 0.05, **p < 0.01. Con, Control group.

2.4 Open Field Test

Open Field Test (OFTs) were conducted on the two groups of mice separately, recording parameters including resting time, average speed, total distance travelled, and distance travelled in the central region during exercise. The methodology of this study was as follows: First, a clean and odorless open-field experimental chamber was prepared, and a camera system (ShXinRuan, XR-XZ301, Shanghai, China) and behavioral analysis software (ShXinRuan, SuperMaze+, Shanghai, China) were set up. The numbers, dates, and other information for the control and AD groups were recorded. Subsequently, for each test, one individual mouse was carefully removed from the feeding cage, and placed in the central area of the experimental box with its back facing the experimenter, after which the experimenter immediately left the study area. Simultaneously, the video capture system was activated to document the mouse movements. The environment remained undisturbed throughout the course of the experiment, which typically lasted for a period of five minutes. At the end of the experiment, mice were returned to their feeding cages, the experimental box was cleaned, and any residual odor was eliminated. Behavioral analysis software was subsequently used to automatically calculate the average speed, total distance, and central area distance of the mice in open fields, thereby enabling the evaluation of their activity range and cognitive levels. Close attention was paid to the standardization of the experimental environment, adaptation period before the experiment, quiet environment during the experiment, and accuracy of data recording throughout the process.

2.5 Hematoxylin and Eosin (HE) Staining

Following necropsy, brain tissues were removed from the mice and fixed in 4% paraformaldehyde. They were



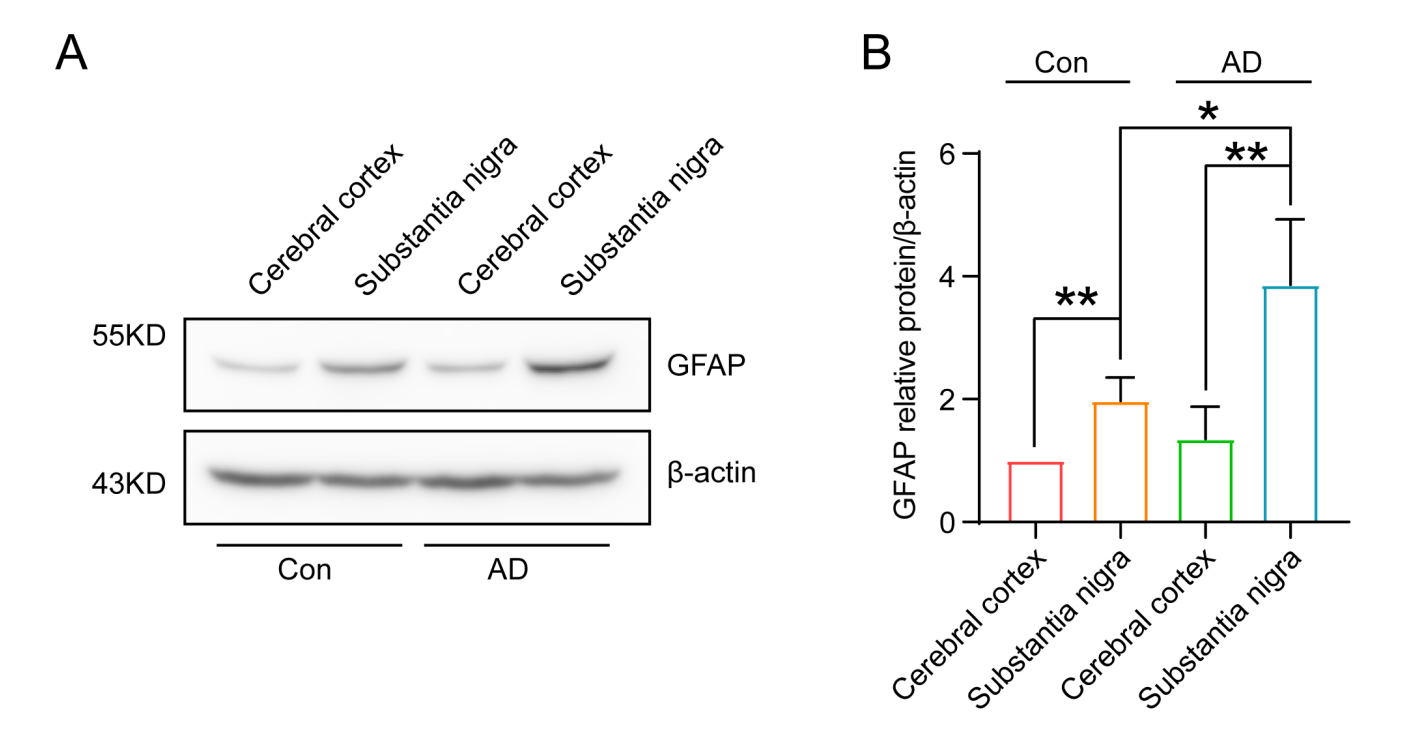


Fig. 2. Significant increase in GFAP content in the substantia nigra region of 71-week-old mice, indicating successful AD modelling. (A) The results of immunoblotting demonstrated a significant elevation of GFAP in the substantia nigra region of the brain of 71-week-old mice. (B) Quantitative analysis of the grey scale values of GFAP expression in the substantia nigra region of the brains of mice in the AD group (A) revealed a significant (n = 3, p < 0.001) increase in the substantia nigra region of 71-week-old mice compared to control 5-week-old mice. Significance symbols indicate: *p < 0.05, **p < 0.01. GFAP, Glial fibrillary acidic protein.

then dehydrated, transparentized, paraffin-embedded and sectioned at a thickness of 5 μ m. The paraffin sections were subsequently baked in an oven at 60 °C for 30 minutes in order to prevent deslaberation. The sections were then dehydrated, stained with hematoxylin for 3–5 minutes, rinsed with running water for 15–30 minutes, re-stained with eosin for 10 s, and again rinsed with running water for 15–30 minutes. Finally, the sections were sealed with neutral gum and morphological changes in the brain tissue sections were observed under a microscope (OLYMPUS BX53, Ishikawamachi, Hachioji-shi, Japan).

2.6 Nissl Staining

Nissl staining was performed based on a previous report [14] with minor modifications. In brief, paraffin sections were sequentially treated with xylene and gradient alcohol, and washed with double-distilled water for 3 min each. The sections were then immersed in a Nissl staining solution for 2–5 minutes, rinsed until the running water was colorless, and observed under a microscope. Differentiation was subsequently performed with appropriate amounts of 0.1% glacial acetic acid, according to the staining results. The slices were then dried and sealed with neutral gum.

2.7 Immunohistochemistry

The immunohistochemistry employed in this study was primarily based on methodologies outlined in a previ-

ous report [15], with minor modifications. In brief, following perfusion with 4% paraformaldehyde, the brain tissue was sliced (at a thickness of 5 μm) following dehydration, transparency, and paraffin embedding. The brain slices were sequentially treated with xylene and a gradient alcohol solution, mixed with citrate buffer for microwave antigen repair, and then titrated with primary antibodies (Tau 1:500, p-Tau 1:100, and Ub-K48 1:200) and incubated in a refrigerator at 4 °C overnight. Subsequently, the slices were incubated with biotin-labelled histochemical secondary antibodies (goat anti-rabbit IgG 1:50, Goat anti-mouse IgG, 1:50). The 3,3'-Diaminobenzidine (DAB) staining solution was finally added. Subsequently, the cells were stained with hematoxylin for 4 min, after which they were rinsed with running water for 15 to 30 min. The slices were then sealed with neutral resin, and analyzed using a microscope (OLYMPUS, BX53, Ishikawa-machi, Hachioji-shi, Japan). The numbers of cells which stained positive for Tau, p-Tau, and Ub-K48 were determined using Image J software (NIH, Image J 1.8.0, Bethesda, MD, USA), and statistical analysis was performed using GraphPad Prism 8.0.1 (Dotmatics, GraphPad Prism 8.0.1, San Diego, CA, USA).

2.8 Western Blot

The experimental mice in each group were anesthetized (1% Pentobarbital sodium (Yacoo, W0091, Suzhou, Jiangsu, China)), after which the brain tissue was



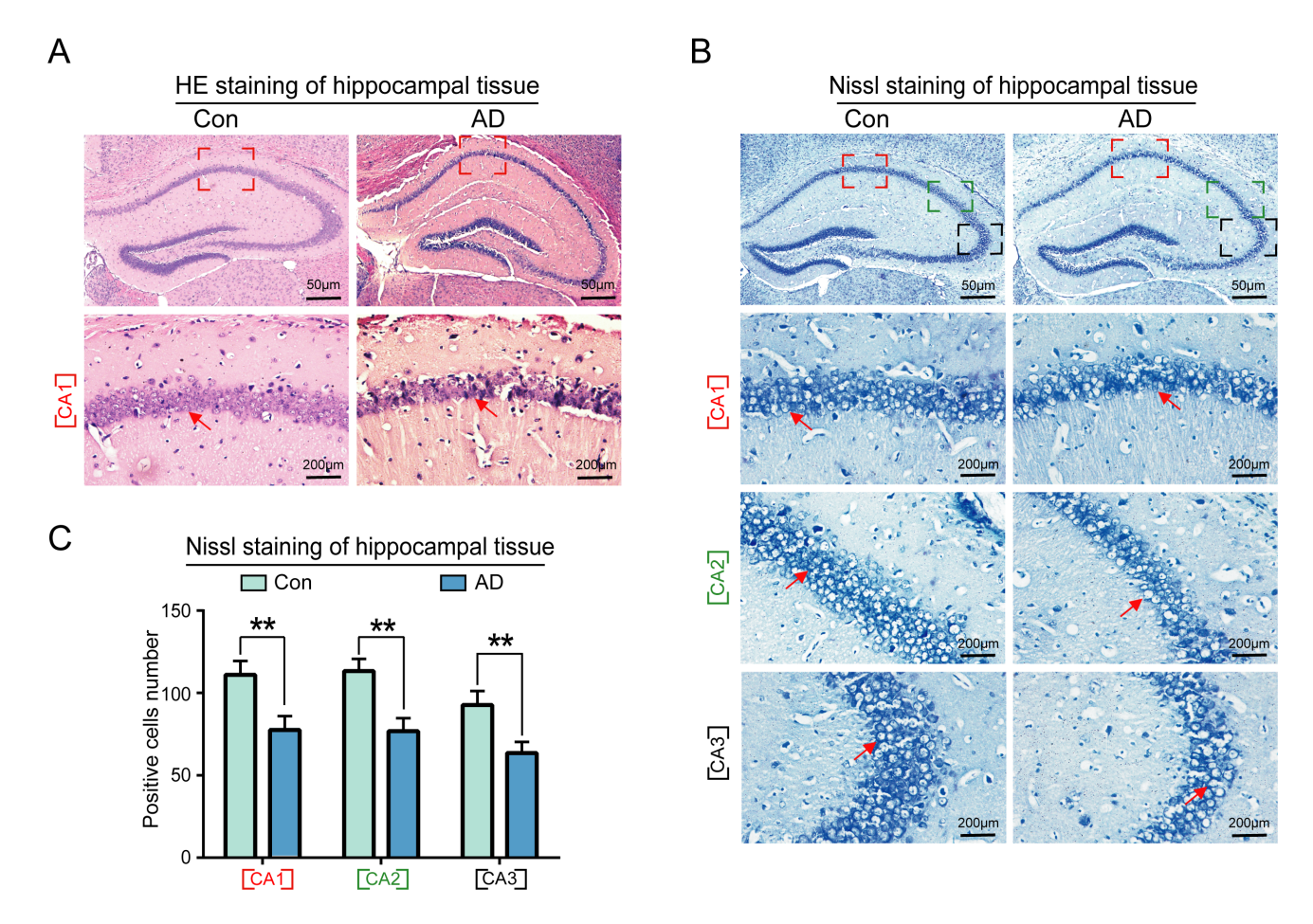


Fig. 3. Morphological and quantitative analysis of neuronal cells in the hippocampus of AD mice. (A) Results of hematoxylin and eosin (HE) staining demonstrated that the neurons in the CA1 area of the hippocampus of the control group mice were neatly arranged, with a regular morphology, rounded nuclei, darker coloring, and tightly packed cells. The cells in the CA1 area of the hippocampus of mice in the AD group exhibited abnormalities, including an irregular and sparse arrangement, large gaps between cells, lighter coloring, and unclear boundaries of the cell and nuclear membranes. (B) Nissl staining further demonstrated a significant reduction in the number of neurons in the CA1, CA2 and CA3 regions of mice in the AD model group. (C) Statistical analysis of Nissl staining results of the AD group compared with the normal group (n = 6, p < 0.01). Significance symbols indicate: **p < 0.01. Scale bar equals 50 μm or 200 μm. The arrows in the Con group refer to normal neuronal cells, while the arrows in the AD group refer to neuronal cells that are abnormally trending towards apoptosis.

exposed and removed. The entire procedure was conducted at a low temperature to prevent protein degradation. The brain tissues were placed in pre-cooled saline and thoroughly washed to remove blood and other impurities. Samples were then weighed on ice and the required quantities of cell lysate and protease inhibitor were added. Subsequently, the brain tissue was thoroughly ground using a tissue homogenizer (BKMAMLAB, BK-HTG80, Changsha, Hunan, China) to obtain a homogenate. In brief, the brain tissue homogenate was sonicated for a duration of three seconds using a sonicator (Tenln, TY-250Y, Yancheng, Jiangsu, China), after which it was incubated on ice for a period of thirty minutes. Subsequently, the brain tissue suspension was subjected to centrifugation at 4 °C (12,000 rpm for 15 minutes) using a high-speed centrifuge. Following centrifugation, the supernatant from

the upper brain tissue protein was carefully aspirated, flash frozen in liquid nitrogen, and stored in an ultra-low temperature refrigerator (Midea, MD86L708, Foshan, Guangdong, China) at $-80~^{\circ}$ C. The extracted proteins were then quantified using a bicinchoninic acid (BCA) protein quantification kit.

Following the extraction of tissue protein, $5 \times SDS$ upsampling buffer was added, and the mixture was heated to 95 °C for denaturation. Subsequently, the proteins in the gel were electrotransferred onto a polyvinylidene difluoride (PVDF) membrane, which was subsequently blocked with skim milk powder for a period of two hours. Subsequently, the membrane was incubated with the primary antibody (GFAP 1:1000; Tau 1:1000; p-Tau 1:1000; Ub-K48 1:1000; Bcl-2 1:1000; Bax 1:500; β -Actin 1:2000; and GAPDH 1:2000) at a temperature of 4 °C for a period of 16



hours. The membrane was then incubated with a secondary antibody (goat anti-rabbit IgG 1:1000; goat anti-mouse IgG 1:1000) at room temperature for 2 h. Use Image J software (NIH, ImageJ 1.8.0, Bethesda, MD, USA) for WB grey value quantification. The initial normalisation of the quantitative results of the WB was achieved by dividing the grey values for the target protein by those of the corresponding internal reference protein (GAPDH or β -actin). This was followed by a second round of normalisation for the target protein, whereby the normalised data for the grey values of the four sets of proteins were divided by the normalised results for the grey values of the target protein in the specially designated control group. And then statistically analyse the data in the graphpad prism software (Dotmatics, GraphPad Prism 8.0.1, San Diego, CA, USA).

2.9 Immunofluorescence

Mouse brains were fixed with formaldehyde, after which the fixed brain tissue was dehydrated using 15% and 30% sucrose. Each dehydration step lasted 48 h. Following dehydration, brain tissues were stored in a -80 °C refrigerator. Frozen brain tissues were sectioned using a microtome. The blades and tissues were kept moist during sectioning to prevent any breakage or curling. Sections were finally placed on clean microscope slides in a box in the dark. Brain slices were washed with Phosphate buffered saline (PBS) to remove the fixative and contaminants, permeabilized with Phosphate-Buffered Saline with Tween 20 (PBST) containing Triton X-100, and blocked with bovine serum albumin (BSA) to minimize any nonspecific staining. After sealing, specific primary antibodies (p-Tau 1:100, Ub-K48 1:200) were added to the brain slices for incubation overnight at 4 °C. The primary antibody was then washed with PBS, after which fluorescein isothiocyanate (FITC)- or tetramethylrhodamine thiocyanate (TRITC)-labeled secondary antibodies were added for incubation at room temperature for 2 h. The nuclei were stained with 2-(4-Amidinophenyl)-6-indolecarbamidine dihydrochloride (DAPI). The brain slices were then washed with PBS, and an anti-quencher was added. Finally, coverslips were added and pressed to remove air bubbles. Sealed slices were finally observed under a fluorescence microscope, and photographs were taken to record and analyze the results. Quantitative statistics of immunofluorescence positive cells were performed by counting positive cells using Image J software (NIH, ImageJ 1.8.0, Bethesda, MD, USA), and the count results were subjected to t-test using Prism software (Dotmatics, GraphPad Prism 8.0.1, San Diego, CA, USA) to calculate the significant difference between each two groups.

2.10 Statistical Analysis

All experimental data were subjected to one-way analysis of variance (ANOVA) in the statistical software SPSS 26.0 (IBM Corp., Armonk, NY, USA), with the results ex-

pressed as mean \pm standard deviation ($\bar{x} \pm s$). Two-by-two comparisons between groups were performed using *t*-test analysis. Statistical significance was set at p < 0.05.

3. Results

3.1 AD Mouse Exhibits Severe Behavioral Abnormalities

SPF grade C57B/L6 mice aged 71-weeks-old were selected as the animal model of AD, while healthy 5-week-old SPF grade C57B/L6 mice were used as the control group. Behavioral assays for the OFT were conducted separately for the two groups of mice. The results of the behavioral tests indicated that AD mice exhibited significantly longer resting times than controls (Fig. 1A,B) (p < 0.05), but significantly lower average speed (Fig. 1C) (p < 0.01), central area distance (Fig. 1D) (p < 0.01), and total distance (Fig. 1E) (p < 0.01), suggesting that AD mice developed cognitive impairment and exhibited abnormal behaviors.

3.2 The Substantia Nigra of AD Mice Exhibited a High Expression of GFAP

Several studies have previously demonstrated that GFAP is indicative of glial cell activation, and thus functions as a valuable diagnostic marker for the early detection of AD. This study employed naturally aged 71-week-old SPF-grade C57BL6 mice as an animal model of AD, with healthy 5-week-old SPF C57BL6 mice serving as the control group. Brain tissues were obtained from six mice in each group, with the substantia nigra region precisely localized, and the expression of GFAP protein in the brain was detected via immunoblotting. The results demonstrated that the substantia nigra region of mice exhibited a high level of GFAP protein expression (Fig. 2A,B) (p < 0.05), indicating the occurrence of AD. For all original Western Blot figures in Fig. 2A, see the Supplementary Materials. This further suggests that the naturally senescent 71-week-old mice in this study were successfully modelled for AD.

3.3 Aberrant Neuronal Cells were Observed in the Hippocampal Region of AD Mice

In this study, the number and morphology of neurons in the hippocampal region of both control and AD groups were observed using hematoxylin and eosin (HE) and Nissl staining. The results of HE staining revealed that the neurons in the CA1 region of the hippocampus of control group mice were neatly and regularly arranged in terms of morphology, while the nuclei of the cells were rounded and full, with darker staining (Fig. 3A, left panel). The cells of the hippocampus in the CA1 region of AD mice exhibited aberrant morphology, disorganized arrangement, and extensive intercellular spaces, with pale staining (Fig. 3A, right panel). The boundaries between the cell and nuclear membranes were not clearly delineated, while the cell nuclei exhibited deep staining and evidence of nuclear rupture in the AD hippocampus (Fig. 3A, right panel).



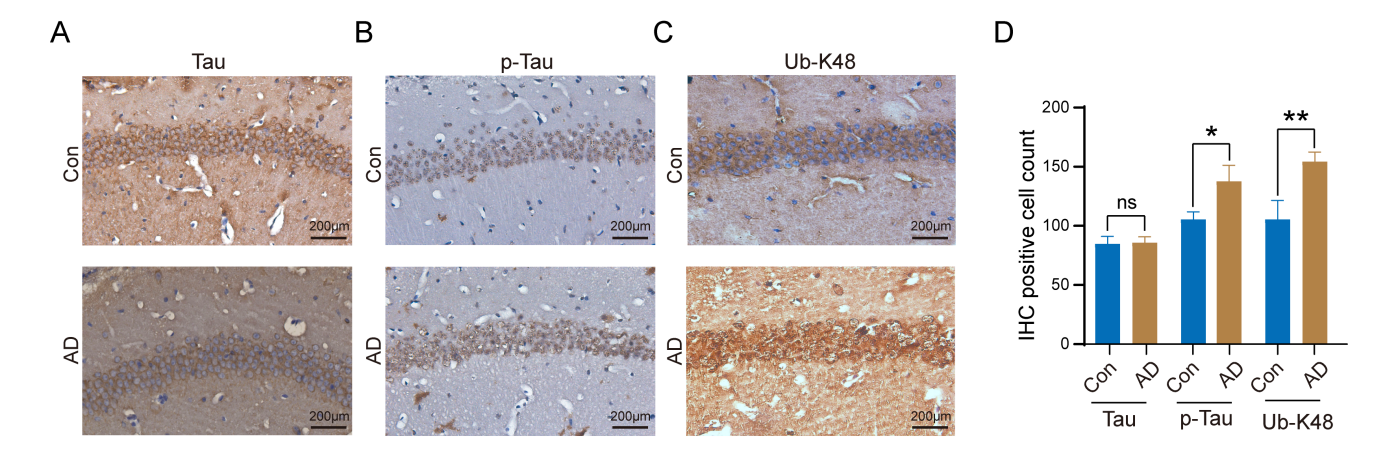


Fig. 4. Increased number of K48-linked ubiquitin chain (Ub-K48) and p-Tau positive cells in the hippocampal region of AD mice. (A) Immunohistochemical staining for Tau protein in the hippocampal region of control and AD mice; (B) Immunohistochemical staining for Phosphorylated Tau (p-Tau) protein in the hippocampal region of control and AD mice; (C) Immunohistochemical (IHC) staining for Ub-K48 in the hippocampus of control and AD mice are shown; (D) Statistical analysis of IHC staining results of the AD group compared with the Con group (p-Tau, n = 6, p < 0.01; Ub-K48, n = 6, p < 0.01). Significance symbols indicate: $^{ns}p > 0.05$, * $^{p}p < 0.05$, * $^{p}p < 0.05$, * $^{p}p < 0.01$. Scale bar equals 200 μm.

Nissl staining revealed a significant reduction in the number of neurons in the CA1, CA2, and CA3 regions of AD mice (Fig. 3B, right panel), as well as a significant reduction in the number of neural progenitor cells in the CA3 region (Fig. 3B, right panel, Fig. 3C) (p < 0.01). These findings were significantly different from those in the normal 5-week group (Fig. 3B, left panel; Fig. 3C) (p < 0.01), indicating that neuronal cells in the hippocampal region of AD mice undergo apoptosis.

3.4 The Hippocampus of AD Mice Exhibited Increased p-Tau and Ub-K48-positive Neuronal Cells

Tau, p-Tau, and Ub-K48 levels in the hippocampal regions of the brains of control and AD mice were examined by immunohistochemistry, with results demonstrating that Tau did not undergo significant changes in neurons within the hippocampal region of AD mice (Fig. 4A). In contrast, we observed a notable increase in the number of neuronal cells that stained positive for p-Tau (Fig. 4B) and Ub-K48 (Fig. 4C), accompanied by a significant increase in their expression levels (Fig. 4D). These findings indicate that p-Tau interacts with Ub-K48, potentially contributing to neuronal apoptosis in the hippocampus.

3.5 Consistent Trends in Protein Expression of p-Tau and Ub-K48 in Hippocampus of AD Mice

Subsequent analyses involved examination of the alterations in the protein expression levels of Tau, p-Tau, and Ub-K48 in the hippocampal regions of the brains of control and AD mice by immunoblotting. The results demonstrated no significant difference in Tau expression in the hippocampus and cortex between normal and AD mice (Fig. 5A,B). In contrast, p-Tau expression was significantly higher in the hippocampal region of AD mice than in the Con group

(Fig. 5C–E) (p < 0.01). Further, we observed Ub-K48 in the hippocampal and cortical regions of both control and AD mice (Fig. 5F), with no significant differences observed between groups (Fig. 5F,G, right panel). The level of Ub-K48 was markedly increased in the hippocampal region of the mouse brain in AD model mice (Fig. 5F,G, left panel) (p < 0.01). For all original Western Blot figures in Fig. 5A,C,F, see the Supplementary Materials. These results were in general agreement with the immunohistochemistry results, and clearly indicated that the lesions in the brains of AD mice are primarily due to the accumulation of Ub-K48 and p-Tau proteins in neuronal cells in the hippocampus. In contrast, the biochemical pathways in other areas of the brain, such as the cortical area, appeared to be similar to those in the normal AD mice (Fig. 5A-G, right panel).

3.6 Co-localization of p-Tau and Ub-K48 in the Hippocampus of AD Mice

We subsequently strived to ascertain the relationship and localization of p-Tau and Ub-K48 in neuronal cells within the hippocampal region. Immunofluorescence double-labeling experiments were performed to ascertain the localization and interrelationship of p-Tau and Ub-K48 in neuronal cells in the hippocampal region, with findings demonstrating that p-Tau and Ub-K48 were co-localized in the hippocampal region of AD mice (Fig. 6). These findings indicated that the formation of Ub-K48 ubiquitin chains may be accompanied by the accumulation of p-Tau.

3.7 The Presence of Apoptotic Markers in the Hippocampal Neuronal Cells of AD Mice

Finally, we sought to ascertain the impact of the accumulation of Ub-K48 and p-Tau proteins on neuronal cells in



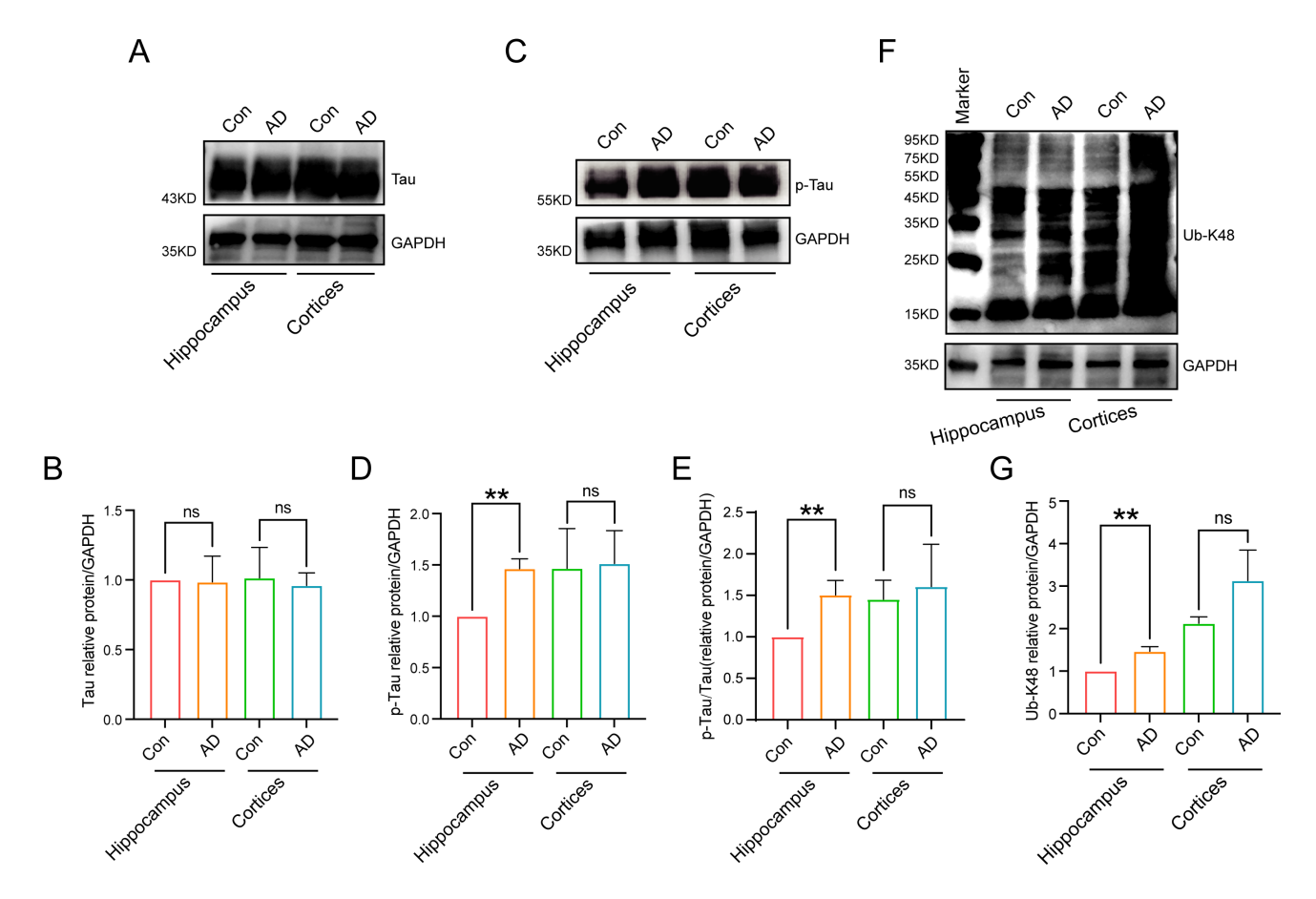


Fig. 5. Protein expression levels in mouse hippocampal regions. (A,B) Tau was expressed in mouse hippocampal and cortical regions, as detected by immunoblotting, with no differences between groups. (C,D) Significant differences in the expression of p-Tau in the AD model groups were observed in the hippocampal region of the mouse brain, as detected by immunoblotting (n = 3, p < 0.01), with no difference observed in the cortical region. (E) Quantitative comparative statistical analysis of the ratio of p-Tau to Tau (n = 3, p < 0.01). (F,G) Ub-K48 was observed in the hippocampal region of the mouse brain, and exhibited a significant elevation in the AD group compared to the control group (n = 3, p < 0.01). Additionally, K48 ubiquitination was observed in the cortical region of the mouse brain in both the normal and AD model groups, although no significant differences were observed. Significance symbols indicate: ^{ns}p > 0.05, **p < 0.01.

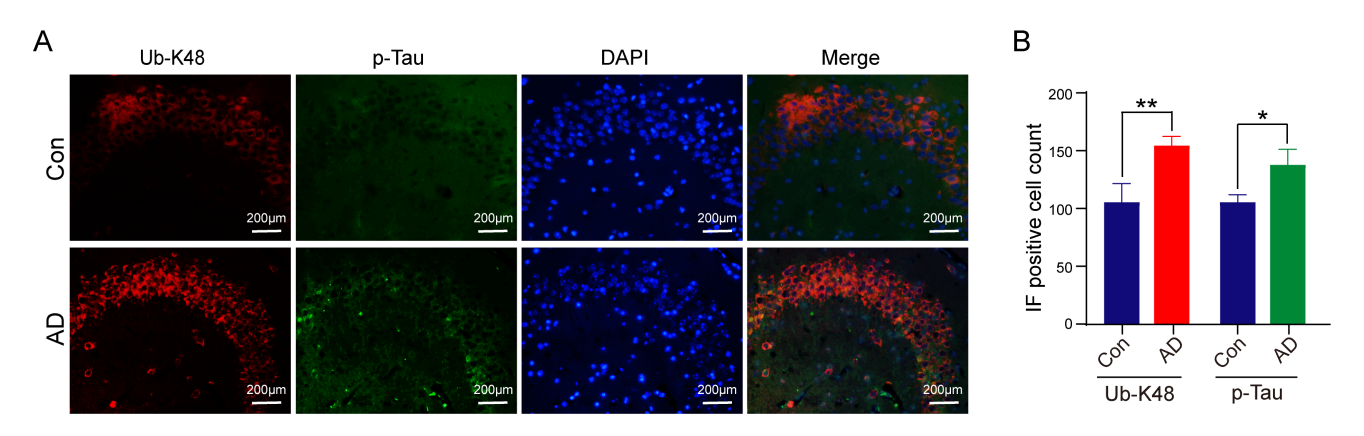


Fig. 6. Immunofluorescence of Ub-K48 and p-Tau-specific antibodies in the hippocampus of mice. (A) Compared with the control group, mice in the AD group showed a significant increase in co-localization of Ub-K48 and p-Tau in the hippocampal region. Scale bar equals 200 μ m. (B) Statistical analysis of Immunofluorescence (IF) staining results of the AD group compared with the Con group (Ub-K48, n = 6, p < 0.01; p-Tau, n = 6, p < 0.05). Significance symbols indicate: *p < 0.05, **p < 0.01. DAPI, 2-(4-Amidinophenyl)-6-indolecarbamidine dihydrochloride.

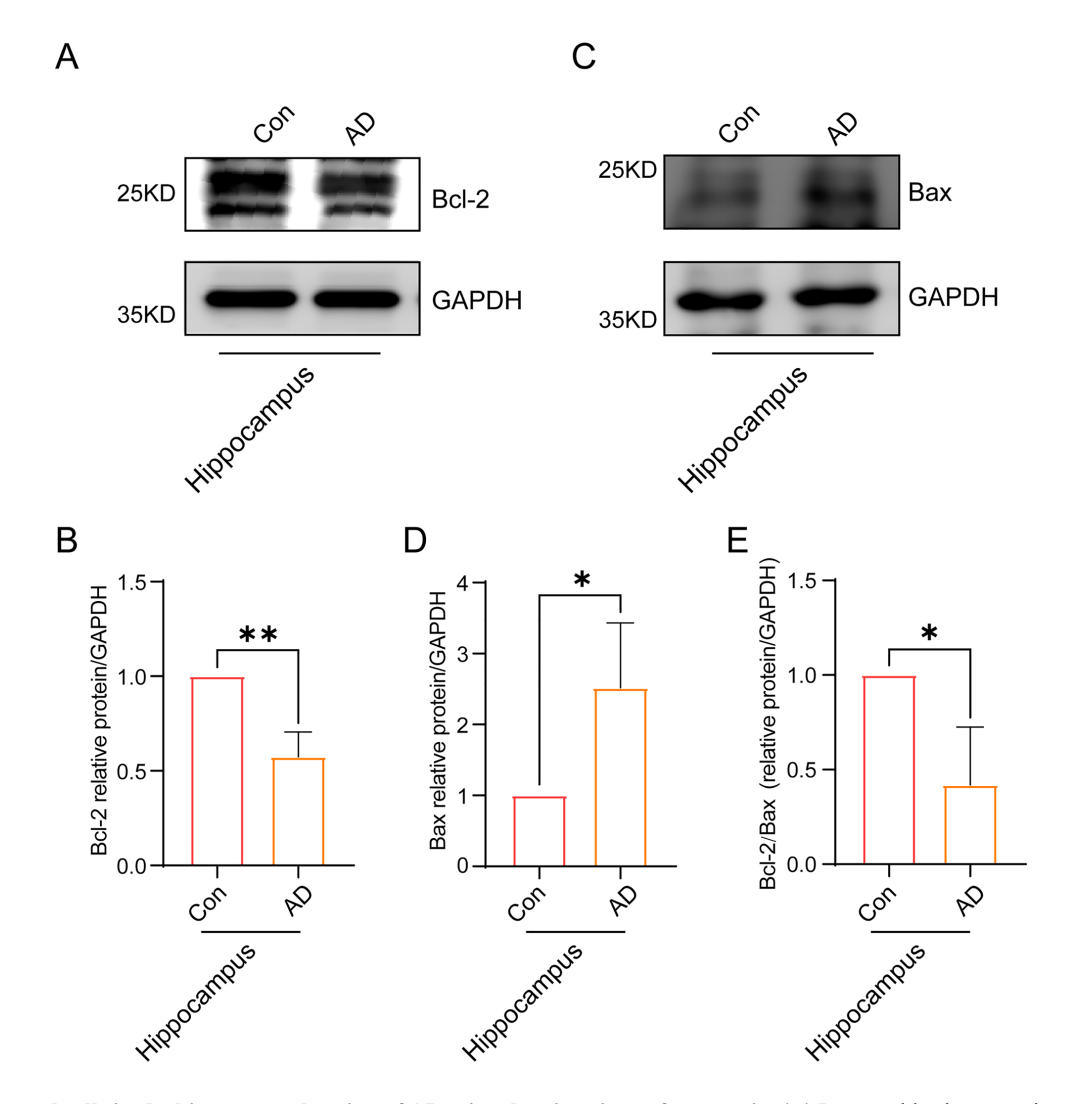


Fig. 7. Neuronal cells in the hippocampal region of AD mice showing signs of apoptosis. (A) Immunoblotting experiments showed a significant reduction in the expression of Bcl-2 in the hippocampal region of the brain in AD mice. (B) A quantitative statistical analysis of grayscale values of immunostained bands in (A) was conducted (n = 3, p < 0.01). (C) Immunoblotting showed an increase in the expression of the pro-inflammatory protein Bax in neuronal cells in the hippocampal region of AD mice. (D) Quantitative statistical analysis of the grayscale values of the immunoblotted bands in (B) (n = 3, p < 0.05). (E) Quantitative comparative statistical analysis of the ratio of Bcl-2 to Bax (n = 3, p < 0.05). Significance symbols indicate: *p < 0.05, **p < 0.01. Bcl-2, B-cell lymphoma-2; Bax, Bcl-2-associated x protein; GAPDH, glyceraldehyde-3-phosphate dehydrogenase.

the hippocampal region of AD mice. The expression of the apoptosis-related factors Bax and Bcl-2 was examined in both the hippocampal and cortical regions of AD mice using immunoblotting. The results demonstrated that the expression of Bcl-2 protein in the hippocampal region of the brains of AD mice decreased (Fig. 7A,B) (p < 0.01), whereas the expression of the pro-inflammatory protein Bax increased (Fig. 7C,D) (p < 0.05). For all original Western Blot figures in Fig. 7A,C, see the **Supplementary Materials**. The Bcl-2/Bax ratio was significantly lower than that in the control group (Fig. 7E) (p < 0.05). These findings indicated that neuronal cells in the hippocampal regions of AD mice underwent inflammation and exhibited signs of apoptosis.

Overall, the above findings collectively delineate a pathway of action orchestrated by the Ub-K48-p-Tau-Bcl-2/Bax pathway in AD pathogenesis. In essence, p-Tau is unable to undergo degradation due to impairment of the UPS, leading to its accumulation in neuronal cells within the hippocampal region of AD. This, in turn, results in a cellular inflammatory response. Subsequently, a substantial quantity of inflammatory factors is released, accompanied by a notable expression of the pro-inflammatory protein Bax. The Bcl-2/Bax ratio was significantly lower than that of the control group, which promoted neuronal cell apoptosis and ultimately contributed to the development of AD (Fig. 8).



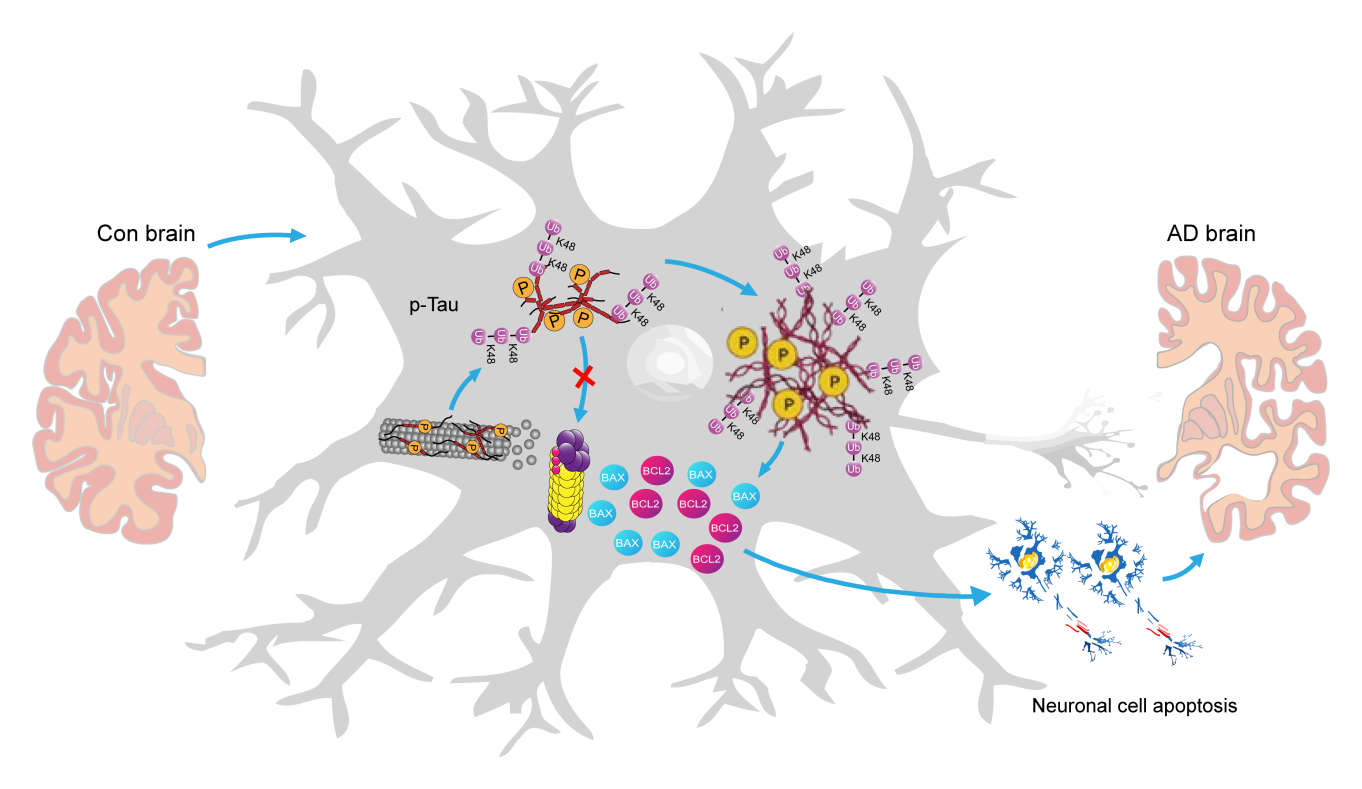


Fig. 8. A graphical summary of the potential mechanistic pathways of the Ub-K48 in AD development. Given that p-Tau cannot be degraded due to damage to the ubiquitin-proteasome system (UPS), it accumulates in the AD hippocampus. This results in the release of numerous inflammatory factors along with Bax and Bcl-2, which promote cell death and contribute to AD. The model drawings for this graphic summary were created using Adobe Illustrator 2020 (Adobe Inc., 24.2, San Jose, CA, USA).

4. Discussion

Abnormal aggregation of p-Tau is a key factor in AD pathogenesis. The formation of NFTs is considered a typical pathological feature of AD, leading to neuronal degeneration, subsequently resulting in learning and memory impairments [16,17]. The study of p-Tau proteins provides the foundation for exploring the treatment of AD lesions. As such, inducing the intracellular degradation of p-Tau proteins and inhibiting their aberrant aggregation may represent an effective method for treating AD [18–20]. The results of the present study demonstrated that neuronal cells in the hippocampal region of mice with AD at 71 weeks of age exhibited aberrant aggregation of p-Tau protein. This finding provides further theoretical support for the hypothesis that aging is a high-risk factor for AD.

The hippocampus is a vital part of the central nervous system, that plays a key role in the acquisition of knowledge and memory retention. Histopathological studies of patients diagnosed with AD have revealed significant neuronal losses and deletions in the hippocampus and cortical areas of the frontal and temporal lobes of the brain. These observations have further identified intracellular neuronal fibrous tangles and granular vacuolar degeneration, which contribute to the gradual deterioration of learning and memory in patients with AD [21,22]. This deterioration can have a profound effect on cognitive function and physical health

[23]. The hippocampal CA regions are initially affected by the deposition of plaques and fibrous tangles during the early stages of AD. Among these regions, damage to the CA3 has been highly correlated with memory and cognitive abilities [24,25]. In the present study, we focused on the pathological changes and neuronal morphology in the hippocampal region (CA1-3) of the brain in a 71-week-old mouse model of AD. Our results suggest that aging is indeed one of an important factor in the development of AD.

The UPS is the primary pathway for intracellular protein degradation, functioning to precisely regulate intracellular protein degradation to maintain normal cellular physiological functions [26]. The complete UPS comprises ubiquitin, ubiquitin-related enzymes (ubiquitin-activating enzyme E1, ubiquitin-conjugating enzyme E2, and ubiquitinligase enzyme E3), deubiquitinating enzymes, the proteasome, and its substrates [27,28]. Perry et al. [29] initially observed a considerable quantity of ubiquitin in the brains of patients, and subsequent study has demonstrated elevated levels of ubiquitin, reduced proteasome activity, and elevated levels of ubiquitin carboxy-terminal hydrolase (UCHL) in the brains of patients with AD [28]. Furthermore, abnormal UCHL expression has been observed, confirming a direct relationship between UPS abnormalities and AD [30,31]. Research has further shown that UCHL-1 in UPS can degrade abnormal Tau proteins in AD brain, while increasing UCHL-1 protein activity can reduce the

deposition of NFTs in the brain [32]. Additionally, diminished UPS function has been postulated to contribute to and exacerbate the progression of neurodegenerative disorders. In the present study, we observed significant aggregation of Ub-K48 and its potential substrate, p-Tau, in neuronal cells in the hippocampal region of the brain in an AD mouse model, suggesting that the UPS proteasome system is defective in neuronal cells. Several drugs targeting different components of the UPS that are currently under development have further demonstrated good clinical efficacy [33–35]. Consequently, the UPS is an important target for the clinical development of potentially effective drugs for AD. The modulation of the UPS pathway is likely to emerge as a new target for future AD [36,37].

It should be noted that the ubiquitination of substrate proteins encompasses both mono-ubiquitination, which is commonly associated with a change in the substrate protein state [38,39], and poly-ubiquitination, which can result in either a change in the substrate protein state, or homeostatic control [40]. With regard to Tau proteins, study has demonstrated that Tau can be ubiquitinated by Ub-K48, -K63, -K6, -K11, and -M1. Ub-K48 is the most prevalent form of ubiquitination and primarily utilizes the ubiquitinproteasome system to degrade Tau [41]. Furthermore, K63 ubiquitination primarily utilizes the autophagic system to regulate Tau protein levels [42]. Additionally, Tau has been shown to decrease the levels of Ub-K6 and Ub-K11, which can impede proteasomal function. Furthermore, Ub-M1, which is linked to neuronal cell death, occurs after Ub-K48 in Tau [41]. Several studies have demonstrated that monoubiquitination of Tau impairs its binding to microtubules, whereas mono-ubiquitination of the N-terminus of Tau may inhibit its aggregation [43,44]. Phosphorylation is one of the most prevalent post-translational modifications of Tau proteins (p-Tau) and can alter the conformation and stability of Tau proteins, consequently affecting their interaction with the ubiquitination system [45]. Phosphorylation can further facilitate the ubiquitination of tau proteins, thereby accelerating their degradation [46]. However, this promotion may be influenced by the phosphorylation site and degree of phosphorylation; further research is required to elucidate the specific type of ubiquitination modification of p-Tau that occurs in AD.

Ub-K48 represents a significant form of ubiquitin chain organization within the UPS, marking proteins for degradation. The present study demonstrated a marked increase in K48 polyubiquitinated chains in the AD hippocampal structural region, accompanied by a marked upregulation of p-Tau. Furthermore, the two proteins showed overlapping intracellular localization in neurons, and were hypothesized to form polymers with each other. In neuronal cells in the hippocampal region of the mouse brain, AD p-Tau protein was labelled and accumulated by Ub-48. It has been postulated that p-Tau cannot be degraded and accumulates in neuronal cells in the hippocampal region of AD due

to damage to the UPS proteasome, which in turn induces a caspase/apoptotic cascade and inflammatory response in the cells. Subsequently, inflammatory factors were released in large quantities, accompanied by a notable expression of pro-inflammatory protein Bax, and the ratio of Bcl-2/Bax was significantly lower than that of the control group, which ultimately promoted neuronal cells to undergo apoptosis. Overall, the present study revealed the reason for the abnormally high expression of Ub-K48 in hippocampal neuronal cells in AD and its mechanism of action in inducing neuronal apoptosis. Subsequent studies will focus on identifying the link between the ubiquitin-proteasome pathway responsible for the accumulation of Ub-K48-tagged p-Tau protein and the signaling pathways of the p-Tau protein that cause apoptosis in cells with a lower ratio of Bcl-2/Bax. A further avenue for future research would be to investigate the correlation between the levels of Ub-K48 and the onset and progression of AD. Additionally, the relationship between Ub-K48 levels and the extent of cognitive differences in the brain associated with neurodegenerative disorders, such as AD, may also be of interest. The findings of this study will facilitate the identification of potential diagnostic and therapeutic targets for neurodegenerative diseases at the epigenetic level, which show enable a clearer understanding of the target and mode of action of this signaling pathway in the process of AD, as well as the exploration of new targets for the effective clinical diagnosis and treatment of AD.

Despite the valuable contributions of this study, it is crucial to note several limitations and opportunities for future refinement. First, the scope of this study did not encompass the potential relationship between Ub-K48 and NFT formation, particularly in relation to Tau. As such, this relationship warrants further exploration, as it may be associated with AD progression. Second, the significant age disparity between the AD model (71-week-old C57BL6 mice) and control (5-week-old mice) may have introduced confounding age-related variables that could have obscured AD-specific effects. Addressing this issue by using agematched mice would strengthen future research. Moreover, the modest sample size of 40 mice limits the generalizability of our findings. Increasing the sample size could consolidate the results and broaden their applicability. Additionally, the study focused on Tau, p-Tau, and Ub-K48 proteins in the hippocampus, while neglecting other markers and pathways associated with AD, which could offer a more holistic view of disease mechanisms. Incorporation of these additional markers is recommended in future studies. Finally, the current study provides only a snapshot of protein expression and behavioral abnormalities at discrete time points. Longitudinal studies may offer valuable insights into the temporal progression of AD and dynamic changes in protein expression, thereby enhancing our understanding of disease mechanisms and progression.



5. Conclusion

In the present study, we found that a large number of misfolded p-Tau proteins that accumulated in hippocampal neuronal cells underwent Ub-K48 modification, which led to inflammation in hippocampal neuronal cells, disrupted the balance of the Bcl-2/Bax signaling pathway, and induced apoptosis, ultimately leading to cognitive deficits in mice with AD. This study reveals the cause of the abnormally high expression of Ub-K48 in hippocampal neuronal cells in AD, and its mechanism of inducing neuronal cell apoptosis. This information should promote the exploration of new targets for the effective clinical diagnosis and treatment of AD of different degrees.

Availability of Data and Materials

All data points generated or analyzed during this study are included in this article and there are no further underlying data necessary to reproduce the results.

Author Contributions

QL, JJ and ZX designed the study; QL and ZX drafted and edited the manuscript; QL, YY and SH acquired and analyzed most of the data; YY, SH, GD, HC, YZ, WF, YH and YT performed the experiments; QL, YY, SH, JJ and ZX contributed to figures preparation and organization. All authors contributed to editorial changes in the manuscript. All authors read and approved the final manuscript. All authors have participated sufficiently in the work and agreed to be accountable for all aspects of the work.

Ethics Approval and Consent to Participate

The animal study was reviewed and approved by the Ethics Committee of Wannan Medical College (WNMC-AWE-2023132).

Acknowledgment

We sincerely thank the editors of the journal and the reviewers for their comments and suggestions. We also thank the laboratory animals sacrificed in this study.

Funding

This work was supported by the Horizontal Scientific Research Project of Wannan Medical College (H202308); Key Natural Science Project of Wannan Medical College (WK2021Z06 and WK2023ZZD11); Natural Science Foundation of Guangdong Province (2020A1515010113); National Natural Science Foundation of China (82072890). Anhui Province Outstanding Youth Research Programme in Colleges and Universities (2024AH020014); The Anhui Province Clinical Medical Research Translation Special Program (202204295107020010 and 202204295107020013).

Conflict of Interest

The authors declare no conflict of interest.

Supplementary Material

Supplementary material associated with this article can be found, in the online version, at https://doi.org/10.31083/j.jin2312223.

References

- [1] Scheltens P, De Strooper B, Kivipelto M, Holstege H, Chételat G, Teunissen CE, *et al.* Alzheimer's disease. Lancet (London, England). 2021; 397: 1577–1590.
- [2] Amemori T, Jendelova P, Ruzicka J, Urdzikova LM, Sykova E. Alzheimer's Disease: Mechanism and Approach to Cell Therapy. International Journal of Molecular Sciences. 2015; 16: 26417–26451.
- [3] Weng FL, He L. Disrupted ubiquitin proteasome system underlying tau accumulation in Alzheimer's disease. Neurobiology of Aging. 2021; 99: 79–85.
- [4] Wu M, Chen Z, Jiang M, Bao B, Li D, Yin X, et al. Friend or foe: role of pathological tau in neuronal death. Molecular Psychiatry. 2023; 28: 2215–2227.
- [5] McKinnon C, De Snoo ML, Gondard E, Neudorfer C, Chau H, Ngana SG, et al. Early-onset impairment of the ubiquitin-proteasome system in dopaminergic neurons caused by α-synuclein. Acta Neuropathologica Communications. 2020; 8: 17
- [6] Li J, Zhu K, Gu A, Zhang Y, Huang S, Hu R, et al. Feedback regulation of ubiquitination and phase separation of HECT E3 ligases. Proceedings of the National Academy of Sciences of the United States of America. 2023; 120: e2302478120.
- [7] Bhat KP, Yan S, Wang CE, Li S, Li XJ. Differential ubiquitination and degradation of huntingtin fragments modulated by ubiquitin-protein ligase E3A. Proceedings of the National Academy of Sciences of the United States of America. 2014; 111: 5706–5711.
- [8] Ibarra-Bracamontes VJ, Escobar-Herrera J, Kristofikova Z, Rípova D, Florán-Garduño B, Garcia-Sierra F. Early but not late conformational changes of tau in association with ubiquitination of neurofibrillary pathology in Alzheimer's disease brains. Brain Research. 2020; 1744: 146953.
- [9] Lazarou M, Sliter DA, Kane LA, Sarraf SA, Wang C, Burman JL, et al. The ubiquitin kinase PINK1 recruits autophagy receptors to induce mitophagy. Nature. 2015; 524: 309–314.
- [10] Robinson EJ, Aguiar S, Smidt MP, van der Heide LP. MCL1 as a Therapeutic Target in Parkinson's Disease? Trends in Molecular Medicine. 2019; 25: 1056–1065.
- [11] Zhao T, Liu C, Liu L, Wang X, Liu C. Aging-accelerated differential production and aggregation of STAT3 protein in neuronal cells and neural stem cells in the male mouse spinal cord. Biogerontology. 2023; 24: 137–148.
- [12] Aghazadeh N, Beilankouhi EAV, Fakhri F, Gargari MK, Bahari P, Moghadami A, et al. Involvement of heat shock proteins and parkin/α-synuclein axis in Parkinson's disease. Molecular Biology Reports. 2022; 49: 11061–11070.
- [13] Cao L, Liu X, Zheng B, Xing C, Liu J. Role of K63-linked ubiquitination in cancer. Cell Death Discovery. 2022; 8: 410.
- [14] Liu M, Wang W, Zhang Y, Xu Z. Effects of combined electroacupuncture and medication therapy on the RhoA/ROCK-2 signaling pathway in the striatal region of rats afflicted by cerebral ischemia. Brain Research Bulletin. 2023; 205: 110828.
- [15] Liu M, Gong R, Ding L, Zhao Y, Yan X, Shi L, *et al.* Gastrodin combined with electroacupuncture prevents the development of



- cerebral ischemia via rebalance of brain-derived neurotrophic factor and interleukin-6 in stroke model rats. Neuroreport. 2024; 35: 664–672.
- [16] Cai Y, Liu J, Wang B, Sun M, Yang H. Microglia in the Neuroinflammatory Pathogenesis of Alzheimer's Disease and Related Therapeutic Targets. Frontiers in Immunology. 2022; 13: 856376.
- [17] Cao Y, Zhang R. The application of nanotechnology in treatment of Alzheimer's disease. Frontiers in Bioengineering and Biotechnology. 2022; 10: 1042986.
- [18] Yang H, Zeng F, Luo Y, Zheng C, Ran C, Yang J. Curcumin Scaffold as a Multifunctional Tool for Alzheimer's Disease Research. Molecules (Basel, Switzerland). 2022; 27: 3879.
- [19] Congdon EE, Sigurdsson EM. Tau-targeting therapies for Alzheimer disease. Nature Reviews. Neurology. 2018; 14: 399– 415.
- [20] Long JM, Holtzman DM. Alzheimer Disease: An Update on Pathobiology and Treatment Strategies. Cell. 2019; 179: 312– 339.
- [21] Uchida, Y., Onda, K., Hou, Z., Troncoso, J. C., Mori, S., Oishi, K. Microstructural Neurodegeneration of the Entorhinal-Hippocampus Pathway along the Alzheimer's Disease Continuum. Journal of Alzheimer's disease. 2023; 95: 1107–1117.
- [22] Lana D, Ugolini F, Giovannini MG. Space-Dependent Glia-Neuron Interplay in the Hippocampus of Transgenic Models of β-Amyloid Deposition. International journal of molecular sciences. 2020; 21: 9441.
- [23] Zhao Z, Liu Y, Ruan S, Hu Y. Current Anti-Amyloid-β Therapy for Alzheimer's Disease Treatment: From Clinical Research to Nanomedicine. International Journal of Nanomedicine. 2023; 18: 7825–7845.
- [24] Cherubini E, Miles R. The CA3 region of the hippocampus: how is it? What is it for? How does it do it? Frontiers in Cellular Neuroscience. 2015; 9: 19.
- [25] Song D, Wang D, Yang Q, Yan T, Wang Z, Yan Y, *et al.* The lateralization of left hippocampal CA3 during the retrieval of spatial working memory. Nature Communications. 2020; 11: 2901.
- [26] Fyfe I. Alzheimer disease-associated gene increases tau pathology. Nature Reviews. Neurology. 2020; 16: 128.
- [27] Al Mamun A, Rahman MM, Zaman S, Munira MS, Uddin MS, Rauf A, et al. Molecular Insight into the Crosstalk of UPS Components and Alzheimer's Disease. Current Protein & Peptide Science. 2020; 21: 1193–1201.
- [28] Jarome TJ, Devulapalli RK. The Ubiquitin-Proteasome System and Memory: Moving Beyond Protein Degradation. The Neuroscientist: a Review Journal Bringing Neurobiology, Neurology and Psychiatry. 2018; 24: 639–651.
- [29] Perry G, Friedman R, Shaw G, Chau V. Ubiquitin is detected in neurofibrillary tangles and senile plaque neurites of Alzheimer disease brains. Proceedings of the National Academy of Sciences of the United States of America. 1987; 84: 3033–3036.
- [30] Banasiak K, Szulc NA, Pokrzywa W. The Dose-Dependent Pleiotropic Effects of the UBB⁺¹ Ubiquitin Mutant. Frontiers

- in Molecular Biosciences. 2021; 8: 650730.
- [31] Mi Z, Graham SH. Role of UCHL1 in the pathogenesis of neurodegenerative diseases and brain injury. Ageing Research Reviews. 2023; 86: 101856.
- [32] Gadhave K, Bolshette N, Ahire A, Pardeshi R, Thakur K, Trandafir C, *et al.* The ubiquitin proteasomal system: a potential target for the management of Alzheimer's disease. Journal of Cellular and Molecular Medicine. 2016; 20: 1392–1407.
- [33] Schmidt MF, Gan ZY, Komander D, Dewson G. Ubiquitin signalling in neurodegeneration: mechanisms and therapeutic opportunities. Cell Death and Differentiation. 2021; 28: 570–590.
- [34] Damgaard RB. The ubiquitin system: from cell signalling to disease biology and new therapeutic opportunities. Cell Death and Differentiation. 2021; 28: 423–426.
- [35] Zhang X, Linder S, Bazzaro M. Drug Development Targeting the Ubiquitin-Proteasome System (UPS) for the Treatment of Human Cancers. Cancers. 2020; 12: 902.
- [36] Bohush A, Bieganowski P, Filipek A. Hsp90 and Its Co-Chaperones in Neurodegenerative Diseases. International Journal of Molecular Sciences. 2019; 20: 4976.
- [37] Wilson DM, 3rd, Cookson MR, Van Den Bosch L, Zetterberg H, Holtzman DM, Dewachter I. Hallmarks of neurodegenerative diseases. Cell. 2023; 186: 693–714.
- [38] Xu Z, Song Z, Li G, Tu H, Liu W, Liu Y, et al. H2B ubiquitination regulates meiotic recombination by promoting chromatin relaxation. Nucleic Acids Research. 2016; 44: 9681–9697.
- [39] Wang L, Xu Z, Wang L, Liu C, Wei H, Zhang R, et al. Histone H2B ubiquitination mediated chromatin relaxation is essential for the induction of somatic cell reprogramming. Cell Proliferation. 2021; 54: e13080.
- [40] Wei Z, Zeng K, Hu J, Li X, Huang F, Zhang B, et al. USP10 deubiquitinates Tau, mediating its aggregation. Cell Death & Disease. 2022; 13: 726.
- [41] Li L, Jiang Y, Wang JZ, Liu R, Wang X. Tau Ubiquitination in Alzheimer's Disease. Frontiers in Neurology. 2022; 12: 786353.
- [42] Puangmalai N, Sengupta U, Bhatt N, Gaikwad S, Montalbano M, Bhuyan A, et al. Lysine 63-linked ubiquitination of tau oligomers contributes to the pathogenesis of Alzheimer's disease. The Journal of Biological Chemistry. 2022; 298: 101766.
- [43] Parolini F, Ataie Kachoie E, Leo G, Civiero L, Bubacco L, Arrigoni G, *et al*. Site-Specific Ubiquitination of Tau Amyloids Promoted by the E3 Ligase CHIP. Angewandte Chemie (International ed. in English). 2023; 62: e202310230.
- [44] Trivellato D, Munari F, Assfalg M, Capaldi S, D'Onofrio M. Untangling the Complexity and Impact of Tau Protein Ubiquitination. Chembiochem: a European journal of chemical biology. 2024; 25: e202400566.
- [45] Rostgaard N, Jul PH, Garmer M, Volbracht C. Increasing O-GlcNAcylation Attenuates tau Hyperphosphorylation and Behavioral Impairment in rTg4510 Tauopathy Mice. Journal of integrative neuroscience. 2023; 22: 135.
- [46] Alquezar C, Arya S, Kao AW. Tau Post-translational Modifications: Dynamic Transformers of Tau Function, Degradation, and Aggregation. Frontiers in Neurology. 2021; 11: 595532.

